










RESEARCH ARTICLE | JANUARY 24 2025

# Tailoring beam profile and OAM spectrum in domain-engineered nonlinear photonic crystals

Special Collection: [Angular Momentum of Light](#)

Xinyu Zhang ; Hangyu Li ; Shiqiang Liu; Yan Chen  ; Zhihan Zhu  ; Hui Liu; Shining Zhu ; Xiaopeng Hu  



APL Photonics 10, 010802 (2025)

<https://doi.org/10.1063/5.0245407>



## Articles You May Be Interested In

Hollow cylindrical three-dimensional nonlinear photonic crystal for annular beam generation

*Appl. Phys. Lett.* (September 2024)

Topological charge transfer in frequency doubling of fractional orbital angular momentum state

*Appl. Phys. Lett.* (October 2016)

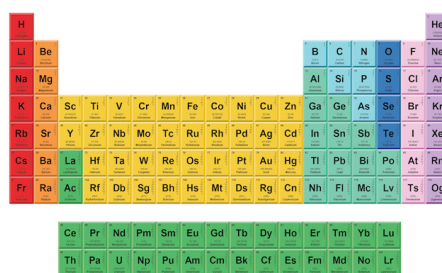
Direct laser poling of lithium niobate on insulator with femtosecond laser

*Appl. Phys. Lett.* (November 2024)



THE MATERIALS SCIENCE MANUFACTURER®

**Now Invent.™**



American Elements  
Opens a World of Possibilities

...Now Invent!

[www.americanelements.com](http://www.americanelements.com)

© 2021-2024 American Elements is a U.S. Registered Trademark

# Tailoring beam profile and OAM spectrum in domain-engineered nonlinear photonic crystals

Cite as: APL Photon. 10, 010802 (2025); doi: 10.1063/5.0245407

Submitted: 26 October 2024 • Accepted: 12 January 2025 •

Published Online: 24 January 2025



Xinyu Zhang,<sup>1</sup> Hangyu Li,<sup>1</sup> Shiqiang Liu,<sup>1</sup> Yan Chen,<sup>2,a)</sup> Zhihan Zhu,<sup>3,a)</sup> Hui Liu,<sup>1,3</sup> Shining Zhu,<sup>1</sup> and Xiaopeng Hu<sup>1,a)</sup>

## AFFILIATIONS

<sup>1</sup> National Laboratory of Solid State Microstructures, College of Engineering and Applied Sciences, and School of Physics, Nanjing University, Nanjing 210093, China

<sup>2</sup> National Key Laboratory of Optical Field Manipulation Science and Technology, Chengdu 610209, China

<sup>3</sup> Wang Da-Heng Center, HLJ Key Laboratory of Quantum Control, Harbin University of Science and Technology, Harbin 150080, China

**Note:** This paper is part of the Special Topic on Angular Momentum of Light.

**a) Authors to whom correspondence should be addressed:** [chenyan@ioe.ac.cn](mailto:chenyan@ioe.ac.cn); [zhuzhihan@hrbust.edu.cn](mailto:zhuzhihan@hrbust.edu.cn); and [xphu@nju.edu.cn](mailto:xphu@nju.edu.cn)

## ABSTRACT

Nonlinear frequency conversion provides a powerful tool to generate and manipulate structured light at new wavelengths. In this work, to meet the demands of applications such as high-capacity optical communications and high-dimensional entanglement generation, we use ferroelectric domain engineering to generate frequency-doubled light beams carrying orbital angular momentum (OAM) superposition states and with adjustable radial intensity distribution. Angular and radial phase modulations were introduced into the modulation function of the second-order nonlinear coefficient distribution of lithium tantalate nonlinear photonic crystals, achieving simultaneous tailoring of the OAM spectrum and the radial intensity profile of the second harmonic (SH) waves. As a representative example, we demonstrate the generation of a SH wave that carries a comb-like OAM spectrum, with the radial intensity distribution concentrating on a ring with a specific radius. In addition, the nonlinear photonic devices developed in this work feature polarization insensitivity and broadband characteristics.

© 2025 Author(s). All article content, except where otherwise noted, is licensed under a Creative Commons Attribution-NonCommercial 4.0 International (CC BY-NC) license (<https://creativecommons.org/licenses/by-nc/4.0/>). <https://doi.org/10.1063/5.0245407>

## I. INTRODUCTION

Nonlinear photonic crystals (NPCs), with 1D to 3D modulation of the quadratic nonlinear susceptibility  $\chi^{(2)}$ ,<sup>1–11</sup> have been proven to be a unique and promising platform to achieve flexible control over various degrees of freedom of the light beams, such as amplitude, phase, and polarization, while obtaining nonlinear frequency conversions. The interaction between light fields and NPCs facilitates the generation of advanced structured light fields at new frequencies, including non-diffracting Airy beams, optical vortices, and spatiotemporal vortex beams.<sup>12–15</sup> Among the research works, the nonlinear generation and manipulation of vortex beams in NPCs, also known as orbital angular momentum (OAM) carrying beams, have garnered significant attention.<sup>16,17</sup> In the past decades, extensive research on vortex beams has covered second harmonic generation (SHG), third harmonic generation (THG), sum frequency

generation (SFG), optical parametric oscillation (OPO), astigmatic transformation, and nonlinear generation from NPCs.<sup>18–27</sup>

Previous studies on the nonlinear generation and manipulation of vortex beams in NPCs have predominantly focused on producing light beams with a single topological charge at new wavelengths. In contrast, there are few studies on the nonlinear generation of the light beam carrying OAM superposition states with the controllable OAM spectrum and the adjustable radial intensity profile. Light beams carrying OAM superposition states with specific wavelengths have important applications in the generation of high-dimensional quantum entangled states, high-capacity optical communications beyond the telecommunication band, and optical micromanipulation (Wang *et al.*).<sup>28–34</sup> For example, the pump light for generating a high-dimensional quantum entangled state requires visible light beams carrying OAM superposition states;<sup>32</sup> light sources carrying the OAM superposition state in the mid-infrared can be obtained

through nonlinear spectral translation based on the commercial telecom band transceiver.<sup>35</sup> For these applications, simultaneously controlling the radial intensity profile is crucial for enhancing imaging resolution, optimizing beam-to-fiber coupling efficiency, and improving micro-particle manipulation.<sup>36–45</sup>

To address the aforementioned demands, in this work, we propose a novel 2D NPC. By modulating both the angular and radial aspects of the  $\chi^{(2)}$  in NPC, we can achieve simultaneous control over the OAM spectrum and the radial intensity profile of the second harmonic (SH) waves.

## II. DESIGN PRINCIPLE

To realize the nonlinear generation of light beams carrying controllably OAM superposition states and simultaneously controlling the radial intensity profiles, we introduce specific angular and radial phase modulation into the  $\chi^{(2)}$ -modulation function of the NPCs, which can be described as the following:

$$\chi^{(2)}(x, y) = d_{ij} \text{sign} \left\{ \cos \left[ \frac{2\pi}{\Lambda} x + \phi_1(\theta) + \phi_2(r) \right] \right\}, \quad (1)$$

where  $d_{ij}$  is an element of the quadratic susceptibility  $\chi^{(2)}$  tensor,  $\Lambda$  is the modulation period in the  $x$ -direction, and  $r$  and  $\theta$  are the radius and azimuth angle of the  $x$ - $y$  plane.  $\phi_1(\theta)$  and  $\phi_2(r)$  are the angular and radial phase modulation functions, respectively. The first-order Fourier component of the nonlinear coefficient is  $F_1 d_{ij} e^{i[2\pi x/\Lambda + \phi_1(\theta) + \phi_2(r)]}$ , where  $F_1$  is the expansion coefficient.

The schematic of the principle is illustrated in Fig. 1. The NPC possesses a 2-D  $\chi^{(2)}$  modulation in the  $x$ - $y$  plane, and it can convert the near-infrared Gaussian-shaped fundamental wave, incident along the  $z$  direction, into the SH visible wave carrying OAM superposition states. During the SHG process in the NPC, nonlinear Raman–Nath diffraction occurs,<sup>7</sup> with the first-order diffraction angle being  $\alpha = \arccos[2\pi/(\Lambda k_z^{\omega})]$ , where  $k_z^{\omega}$  is the wave vector of the SH wave. According to the Green's function theory, the complex amplitude of SH wave can be described as

$$E^{(2\omega)} \propto L \sin c \left( \frac{dk_z L}{2} \right) \iint E^{(\omega)2} e^{i\phi_1(\theta) + i\phi_2(r)} e^{ik_r^{\omega} r \cos(\theta - \varphi)} r d\theta dr, \quad (2)$$

where  $dk_z = k_z^{2\omega} \cos \alpha - 2k_z^{\omega} - k_r^{\omega} \sin \alpha \cos \varphi$  is the  $z$ -component wave vector mismatch,  $k_z^{\omega}$  and  $k_z^{2\omega}$  are the wave vectors of the fundamental wave and the SH wave along the propagation direction, respectively.  $k_r^{\omega}$  is the transverse wave vector of the SH wave, and  $r'$  and  $\varphi$  are the radius and azimuth angle in the  $x'$ - $y'$  plane.  $L$  is the thickness of the NPC, and  $E^{(\omega)}$  is the complex amplitude of the fundamental wave. In Eq. (2),  $e^{i\phi_1(\theta)} = \sum_{\ell} c_{\ell} e^{i\ell\theta}$  the expansion coefficient is  $c_{\ell} = \frac{1}{2\pi} \int e^{i\phi_1(\theta)} e^{-i\ell\theta} d\theta$ , and  $\ell$  denotes the topological charge. The complex amplitude of the SH wave can be derived,

$$E^{(2\omega)} \propto \sum_{\ell} c_{\ell} u_{\ell}(k_r^{\omega}) e^{i\ell\varphi}, \quad (3)$$

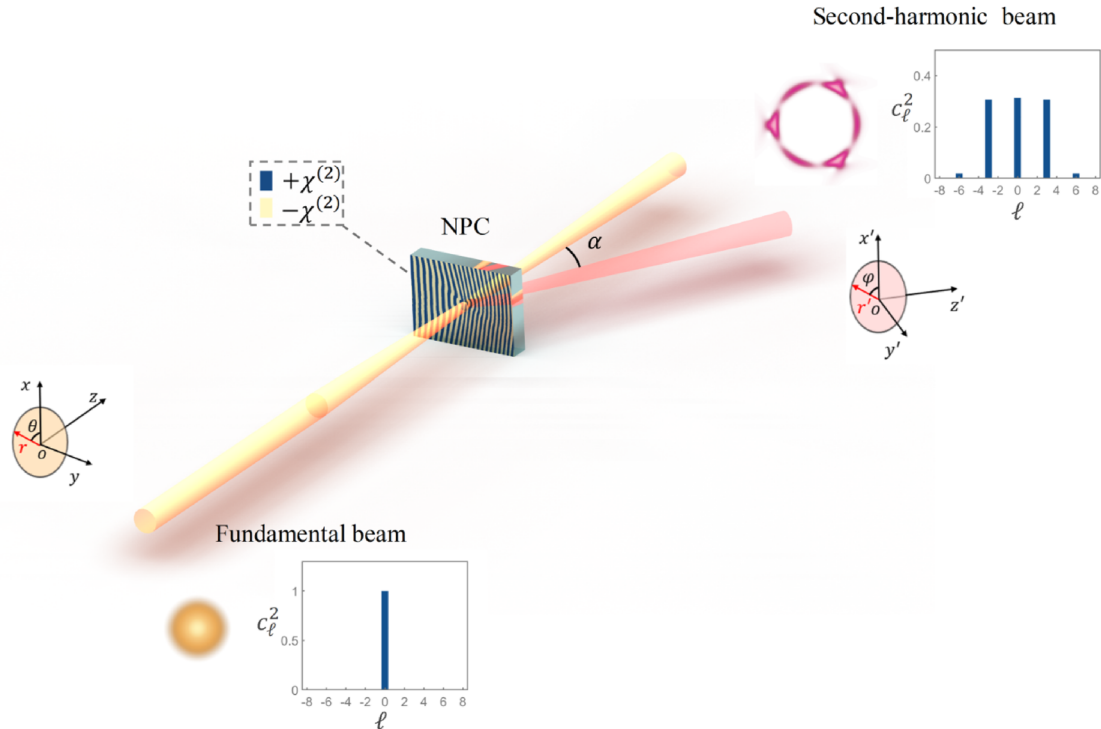


FIG. 1. Schematic diagram of nonlinear generation of light beams carrying controllably OAM superposition states and adjustable radial intensity profiles.

where  $u_\ell(k_r^{2\omega}) = \int E^{(\omega)^2} e^{i\phi_2(r)} J_\ell(k_r^{2\omega} r) r dr$ ,  $J_\ell(k_r^{2\omega} r)$  is the first Bessel function of  $\ell$ -order (supplementary material 1). From Eq. (3), we can see that the complex amplitude of the SH wave  $E^{(2\omega)}$  contains a series of OAM states with various complex weights  $c_\ell$ , and  $|c_\ell|^2$  represents the intensity of each OAM component. Due to the conjugate relationship between the azimuthal angle and OAM, the Fourier transform of the angular phase function,  $\phi_1(\theta)$ , can be employed to derive the OAM spectrum of the SH wave. In contrast, the radial phase modulation function  $\phi_2(r)$  is independent of the angular phase modulation function  $\phi_1(\theta)$  and solely influences the radial intensity profile of the SH wave, without affecting its OAM spectrum. Therefore, we can control the OAM spectrum and the radial intensity profile of the SH wave by independently modulating the angular and radial phase modulation function of  $\chi^{(2)}$ .

### III. RESULTS AND DISCUSSIONS

Figure 2 shows the schematic experimental setup for nonlinear generation and manipulation of light beams carrying OAM superposition states. The fundamental wave from a regenerated and amplified Ti:sapphire laser, which exhibits a Gaussian profile, delivers 150 fs pulses at a repetition frequency of 5 KHz, and the working wavelength is 1300 nm. The near-infrared fundamental wave was converted into vertical polarization by a half-wave plate and then was focused into a 0.5 mm-thick NPC with a lens L1 ( $f = 200$  mm). Nonlinear Roman–Nath diffraction occurred via the type-0 SHG process, and the +1st order SH wave was selected using an aperture and subsequently divided by a beam splitter (BS) for measuring the intensity profile and OAM spectrum, respectively. The residual fundamental wave was filtered out using a filter. The transmitted SH wave through the BS was recorded with a CCD camera in the

Fourier plane of lens L2 ( $f = 150$  mm) to capture the intensity profile of the SH wave. To measure the OAM spectrum, the SH wave reflecting from the BS was incident onto a spatial light modulator (SLM), and a series of helical phase holograms were loaded onto the SLM. Only the specific OAM component of the SH wave that has a conjugate spiral phase with the known single spiral phase loaded on the SLM can be converted into a fundamental Gaussian mode in the Fourier plane of the reflected field. The intensity of the restored Gaussian mode, which was measured with a power meter, represents the weight of the corresponding OAM component, while other OAM components maintain their ring-shaped intensity distribution surrounding the fundamental Gaussian mode.<sup>46</sup>

To verify the design method, we introduced two different angular phase modulation functions into the NPCs:  $\phi_1(2\theta) = \pi \text{sign}[\cos(2\theta)]$  and  $\phi_1(3\theta) = \pi \text{sign}[\cos(3\theta)]$ . In addition, two angular phase modulation functions were taken into consideration: one does not have radial phase modulation, i.e.,  $\phi_2(\rho) = 0$ , and the other has radial phase modulation,  $\phi_2(\rho) = \rho r$ , where  $\rho = \pi/40 \mu\text{m}^{-1}$ . The designed structures of the NPC, the microscopic images of the fabricated NPC, along with the patterns and OAM spectra of the generated SH waves, are shown in Fig. 3. We can see from the microstructure of the NPC shown in Figs. 3(a) and 3(c) that in the absence of radial phase modulation, the NPC exhibits angular periodic modulation superimposed on a 1D periodic structure, the modulation period being  $2\pi/m$ , ( $m = 2, 3$ ). The intensity profiles of SH waves display a petal-like structure with the number of petals being  $2m$ , corresponding to twice that of the angular periodicity. The OAM spectrum of SH wave predominantly contains OAM components with topological charge, which are odd multiples of the angular phase modulation period  $m$ , and the weight of the OAM components decreases with the order increasing. The

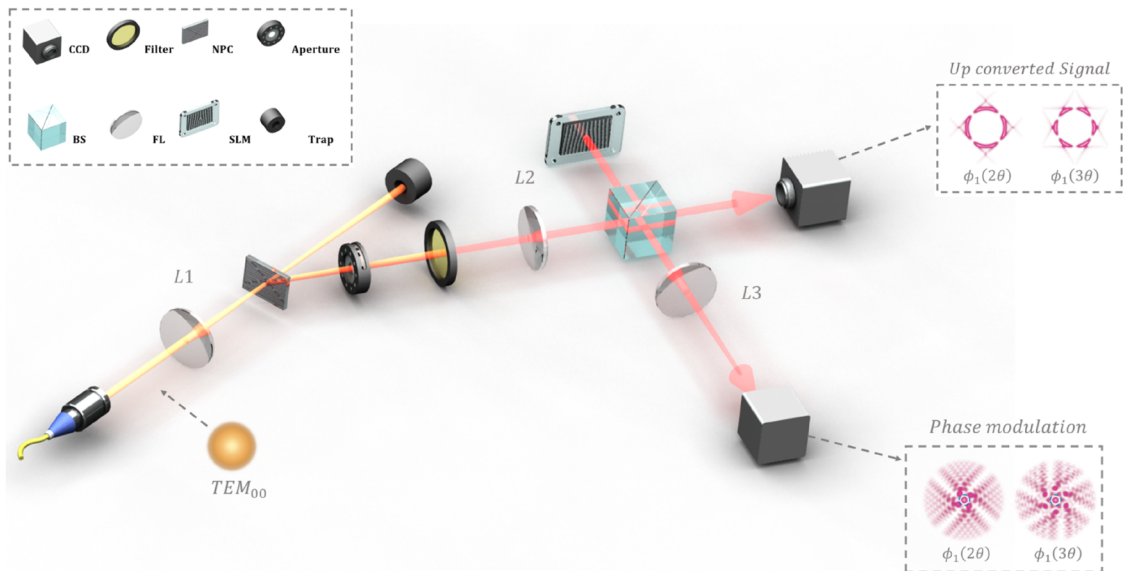


**FIG. 2.** Schematic illustration of the experimental setup. The intensity profiles of the SH waves were shown in the upper right inset. The OAM spectra of SH waves were measured via phase modulation as shown in the bottom right inset, where the center patterns surrounded by blue dashed circles are the intensity of the restored OAM component.



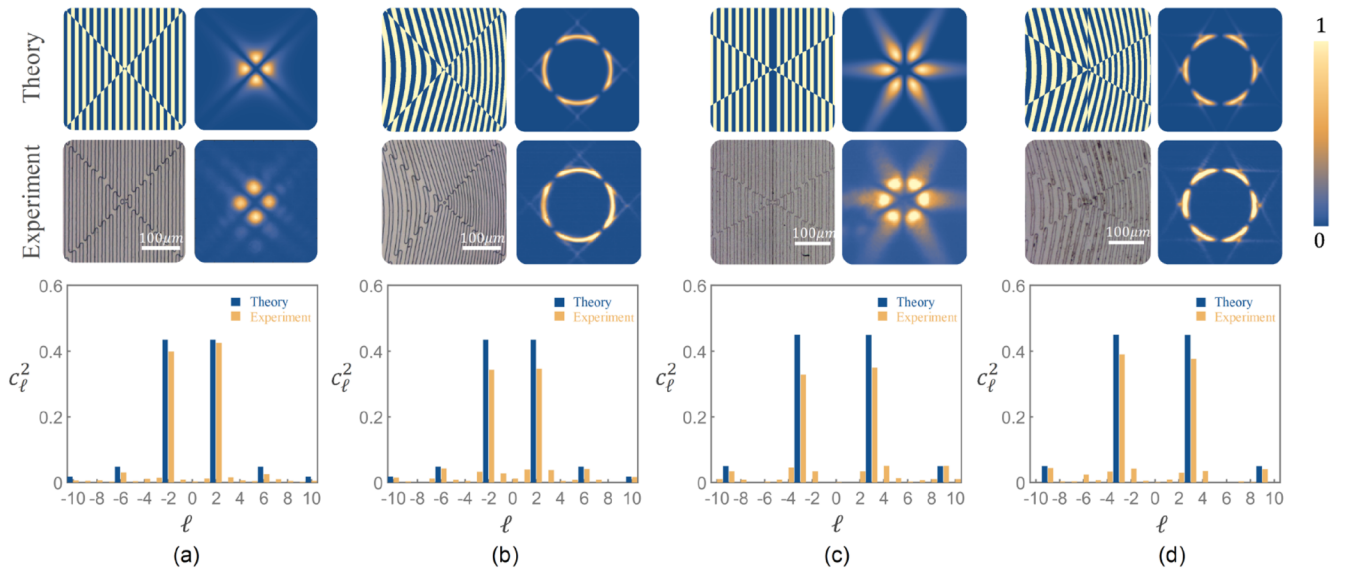


**FIG. 3.** Micro-structure of the NPC, the intensity profile, and the OAM spectrum of the generated SH wave for different combinations of the modulation functions: (a)  $\phi_1(2\theta)$  without the radial phase modulation, (b)  $\phi_1(2\theta)$  and  $\phi_2(\rho)$ , (c)  $\phi_1(3\theta)$  without the radial phase modulation, and (d)  $\phi_1(3\theta)$  and  $\phi_2(\rho)$ , where  $\phi_1(2\theta) = \pi \text{sign}[\cos(2\theta)]$ ,  $\phi_1(3\theta) = \pi \text{sign}[\cos(3\theta)]$ , and  $\phi_2(\rho) = \rho r$  ( $\rho = \pi/40 \mu\text{m}^{-1}$ ).

theoretical OAM spectrum distribution is obtained by performing a Fourier transform on  $\phi_1(m\theta)$ , and the details can be found in [supplementary material 2](#). When the radial phase modulation is introduced, the NPC structure exhibits curved domain patterns, and the intensity profile of the SH wave transforms into an uneven ring-like structure. The calculated and experimentally measured OAM spectra are consistent with OAM spectra without radial phase modulation, as shown in [Figs. 3\(b\) and 3\(d\)](#).

In principle, our design strategy can generate SH waves with arbitrary OAM spectra and adjustable radial intensity profiles. As an example, we designed to generate SH OAM-comb with five equal-weighted and equal-spaced OAM components at  $\ell = -4, -2, 0, 2, 4$ . The angular phase modulation function  $\phi_{opt}(\theta)$  was obtained using a global search algorithm ([supplementary material 3](#)), and the radial phase modulation was set to be  $\phi_2(\rho r) = \rho r$ , where  $\rho = \pi/40 \mu\text{m}^{-1}$ . The calculated and measured SH wave intensity profile and OAM spectrum are shown in [Fig. 4\(a\)](#). The SH wave intensity profile is concentrated at a specific radial position, forming an uneven ring-like structure with four bright spots along the ring, where the emission angle is calculated to be about  $0.17^\circ$ . The measured OAM spectrum is consistent with the calculations, and the fidelity<sup>47</sup> is 0.95. The discrepancy is primarily attributed to the fabrication errors of the NPC. Our proposal for OAM-comb generation can be easily expanded to a much larger OAM space. The minimum size of the inverted domain in our study is  $10 \times 10 \mu\text{m}^2$ . With the increasing of the OAM space, smaller ferroelectric domain structures will be introduced into the NPCs. When the smallest size of an inverted domain reaches sub-micron or below, it is challenging in fabrication using the conventional electric field poling technique, and the femto-second laser nano-printing technique<sup>10</sup> may be a solution.

It is worth noting that the radial phase modulation  $\phi_2(\rho r) = \rho r$  is equivalent to the phase of an axicon, where  $\rho$  is the cone parameter, enabling the generation of a perfect vortex beam and, therefore, controlling the radial intensity profile of the beam. To investigate the radial intensity profile of the SH wave with different OAM spectra under the same radial phase modulation, we performed numerical simulations with a fixed radial phase modulation function  $\rho = \pi/40 \mu\text{m}^{-1}$  and different angular phase modulation functions, as shown in [Fig. 4\(b\)](#). We found that for the same radial modulation function, the intensity profile of the frequency-doubled light is concentrated in the same radial region, regardless of whether the frequency-doubled light carries a single topological charge or a superposition state of OAM.

The NPC in our work features polarization insensitivity and broadband characteristics. The host material for the NPC is congruent lithium tantalate, which exhibits isotropic refractive indices in the  $x-y$  plane. In the experiment, the fundamental wave was incident along the optical axis ( $z$ -direction) of the crystal, and Type-0 (oo-o) SHG occurred. The generated SH wave will diffract along certain directions rather than the optical axis, and this is attributed to the non-collinear nature of the nonlinear Raman-Nath phase matching diagram. In the coordinate system of the fundamental wave, the polarization of the SH wave did vary with the noncollinear angle; however, in the study, the SH beams were characterized at the plane perpendicular to the nonlinear diffraction direction instead of the optical axis. According to our observations during the experiment, the intensity profiles of the generated SH waves kept almost the same while tuning the polarization of the fundamental wave. Moreover, the NPC demonstrated the broadband in the experiment; when the wavelength of the fundamental wave was set to be 1300, 1060, 1000, and 800 nm, the

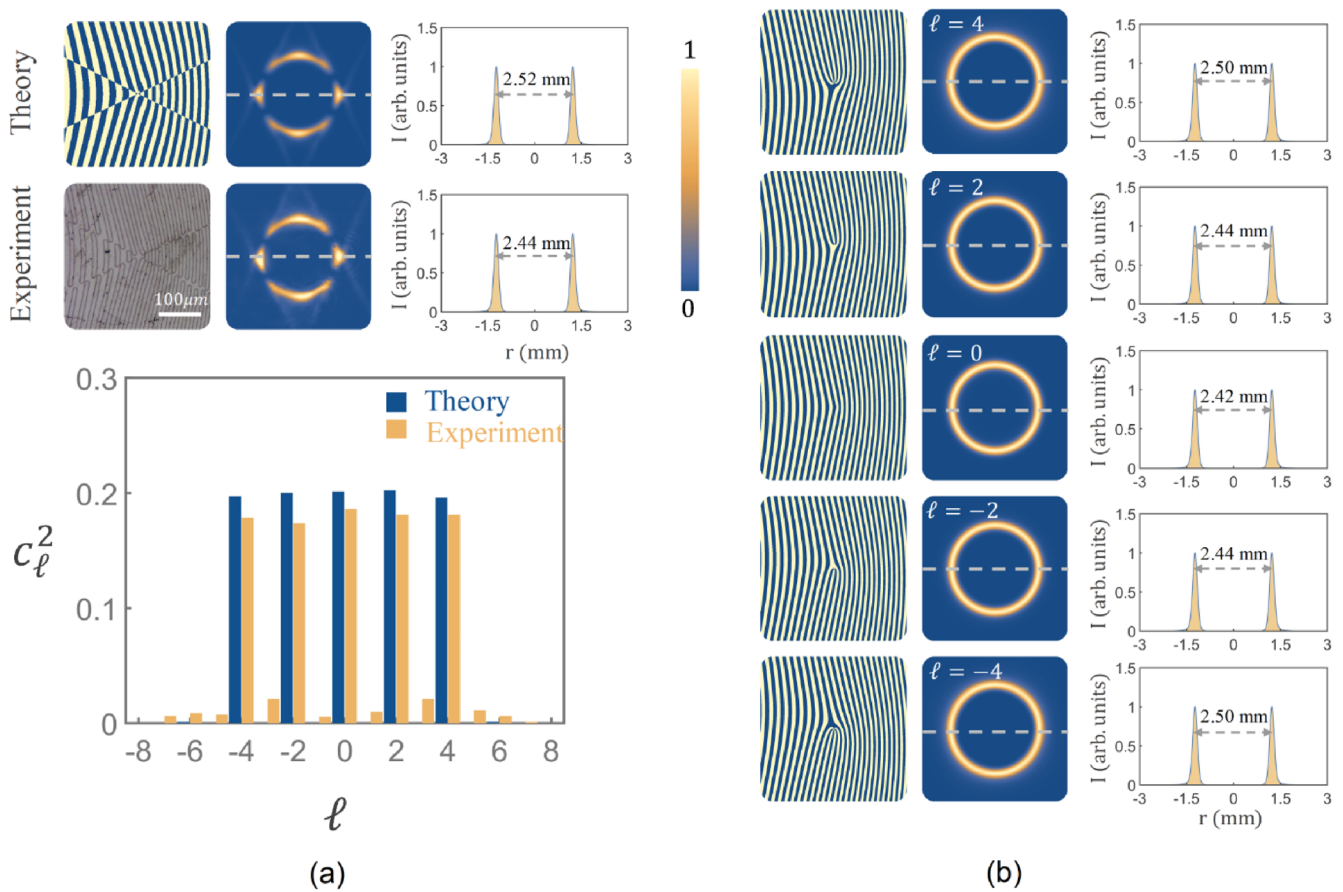


**FIG. 4.** Controlled generation of SH waves with arbitrary OAM spectrum and adjustable radial intensity profile. (a) The designed structure of the NPC, the microscopic image of the fabricated NPC, along with the intensity profile and OAM spectrum of the generated SH wave. (b) The simulation structures of the NPCs, the intensity profiles, and the diameters of the SH waves with different single topological charges  $\ell$ .

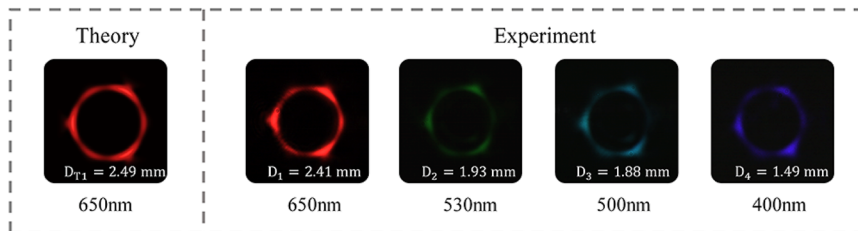


**FIG. 5.** Intensity profiles of the generated SH waves with different wavelengths of the fundamental wave, and the diameter of every ring is indicated.

captured SH wave intensity profiles remained unchanged, and the diameter of the generated SH ring decreased as the fundamental wave was tuned to shorter wavelengths, as shown in Fig. 5. According to Eq. (2), the conversion efficiency is proportional to  $L^2$  and is modulated by the  $\sin^2(dk_z L/2)$  term, which oscillates with the thickness  $L$ . The intensity profile and the OAM spectrum of the SH beam will remain almost unchanged when the thickness of the nonlinear photonic crystal is in the order of several millimeters.<sup>48</sup>

#### IV. CONCLUSIONS

To conclude, we have proposed a scheme to achieve the controllable generation of OAM spectrum and radial intensity distribution of the SH wave from NPCs. Through ferroelectric domain engineering, that is, introducing angular and radial phase modulation into the modulation function of the second-order nonlinear coefficient of the NPCs, the OAM spectrum and the beam radial intensity distribution can be controlled independently. We designed different groups of angular and radial phase modulation functions

and fabricated the corresponding NPCs and verified the feasibility of the proposed scheme by investigating the OAM spectrum and intensity distribution of the SH waves. Furthermore, we used a global search algorithm to generate an optimized angular modulation function to achieve the nonlinear generation of OAM-comb, in which the five components  $\ell = -4, -2, 0, 2, 4$  are equal-weighted and equal-spaced. Meanwhile, the radial phase modulation can make the OAM-comb carrying beam concentrate on a ring of a specific radius, regardless of the OAM spectra. For the NPC in this study, the fundamental wave is incident along the  $z$  optical axis of the congruent lithium tantalite crystal. Due to the isotropy of lithium tantalate in the  $x$ - $y$  plane, the nonlinear device also exhibits polarization insensitivity and wavelength broadband operation. The proposed scheme in this work will lay the foundation for applications in areas such as high-dimensional entangled photon generation, high-capacity communications across different wavelength bands, and optical micromanipulation.

## SUPPLEMENTARY MATERIAL

See the [supplementary material](#) for detailed derivations of Eq. (2), Fourier transform derivations of the angular phase distributions corresponding to Fig. 3, and the principles of algorithms used to optimize the angular phase distributions corresponding to specific OAM spectra.

## ACKNOWLEDGMENTS

This work was supported by the National Key Research and Development Program of China (Grant Nos. 2022YFA1205100 and 2022YFF0712800), the National Natural Science Foundation of China (Grant Nos. 12174185, 12474324, 12192251, 12204483, 92163216, 92150302, and 62288101), and the Postgraduate Research & Practice Innovation Program of Jiangsu Province (Grant No. KYCX24\_0132).

## AUTHOR DECLARATIONS

### Conflict of Interest

The authors have no conflicts to disclose.

## Author Contributions

**Xinyu Zhang:** Data curation (equal); Investigation (equal); Writing – original draft (equal). **Hangyu Li:** Data curation (supporting); Investigation (supporting). **Shiqiang Liu:** Data curation (supporting); Investigation (supporting). **Yan Chen:** Conceptualization (equal); Investigation (equal). **Zhihan Zhu:** Conceptualization (equal); Writing – review & editing (equal). **Hui Liu:** Conceptualization (equal); Funding acquisition (equal). **Shining Zhu:** Funding acquisition (equal). **Xiaopeng Hu:** Conceptualization (equal); Funding acquisition (equal); Writing – review & editing (equal).

## DATA AVAILABILITY

The data that support the findings of this study are available from the corresponding authors upon reasonable request.

## REFERENCES

- S. Zhu, Y. Zhu, and N. Ming, *Science* **278**(5339), 843–846 (1997).
- X. Hu, Y. Zhang, and S. Zhu, *Adv. Mater.* **32**(27), e1903775 (2020).
- W. T. Buono and A. Forbes, *Opto-Electron. Adv.* **5**(6), 210174 (2022).
- V. Berger, *Phys. Rev. Lett.* **81**(19), 4136 (1998).
- Y. Qin, C. Zhang, Y. Zhu, X. Hu, and G. Zhao, *Phys. Rev. Lett.* **100**(6), 063902 (2008).
- S. M. Saltiel, D. N. Neshev, R. Fischer, W. Krolikowski, A. Arie, and Y. S. Kivshar, *Phys. Rev. Lett.* **100**(10), 103902 (2008).
- N. V. Bloch, K. Shemer, A. Shapira, R. Shiloh, I. Juwiler, and A. Arie, *Phys. Rev. Lett.* **108**(23), 233902 (2012).
- A. Shapira, R. Shiloh, I. Juwiler, and A. Arie, *Opt. Lett.* **37**(11), 2136–2138 (2012).
- D. Wei, C. Wang, X. Xu, H. Wang, Y. Hu, P. Chen, J. Li, Y. Zhu, C. Xin, X. Hu *et al.*, *Nat. Commun.* **10**(1), 4193 (2019).
- X. Xu, T. Wang, P. Chen, C. Zhou, J. Ma, D. Wei, H. Wang, B. Niu, X. Fang, D. Wu *et al.*, *Nature* **609**(7927), 496–501 (2022).
- D. Wei, C. Wang, H. Wang, X. Hu, D. Wei, X. Fang, Y. Zhang, D. Wu, Y. Hu, J. Li, S. Zhu, and M. Xiao, *Nat. Photonics* **12**(10), 596–600 (2018).
- T. Ellenbogen, N. Voloch-Bloch, A. Ganany-Padowicz, and A. Arie, *Nat. Photonics* **3**(7), 395–398 (2009).
- X. Hong, B. Yang, C. Zhang, Y. Qin, and Y. Zhu, *Phys. Rev. Lett.* **113**(16), 163902 (2014).
- X. Hu, S. Liu, T. Xu, Y. Sheng, R. Zhao, and W. Krolikowski, *Opt. Lett.* **48**(21), 5527–5530 (2023).
- S. Liu, X. Zhang, H. Chen, H. Xie, S. Yang, S. Zhu, and X. Hu, *Opt. Lett.* **48**(22), 5951–5954 (2023).
- Y. Shen, X. Wang, Z. Xie, C. Min, X. Fu, Q. Liu, M. Gong, and X. Yuan, *Light: Sci. Appl.* **8**(1), 90 (2019).
- C. He, Y. Shen, and A. Forbes, *Light: Sci. Appl.* **11**(1), 205 (2022).
- J. Pan, H. Wang, Z. Shi, Y. Shen, X. Fu, and Q. Liu, *Appl. Phys. Lett.* **125**(9), 091107 (2024).
- H.-J. Wu, B.-S. Yu, Z.-H. Zhu, W. Gao, D.-S. Ding, Z.-Y. Zhou, X.-P. Hu, C. Rosales-Guzmán, Y. Shen, and B.-S. Shi, *Optica* **9**(2), 187–196 (2022).
- R. Ni, Y. Niu, L. Du, X. Hu, Y. Zhang, and S. Zhu, *Appl. Phys. Lett.* **109**(15), 151103 (2016).
- X. Fang, D. Wei, D. Liu, W. Zhong, R. Ni, Z. Chen, X. Hu, Y. Zhang, S. Zhu, and M. Xiao, *Appl. Phys. Lett.* **107**(16), 161102 (2015).
- Z. Xu, Z. Lin, Z. Ye, Y. Chen, X. Hu, Y. Wu, Y. Zhang, P. Chen, W. Hu, Y. Lu *et al.*, *Opt. Express* **26**(13), 17563–17570 (2018).
- N. A. Chaitanya, A. Aadhi, M. Jabir, and G. K. Samanta, *Opt. Lett.* **40**(11), 2614–2617 (2015).
- K. Shemer, N. Voloch-Bloch, A. Shapira, A. Libster, I. Juwiler, and A. Arie, *Opt. Lett.* **38**(24), 5470–5473 (2013).
- V. Sharma, G. Samanta, S. C. Kumar, R. Singh, and M. Ebrahim-Zadeh, *Opt. Lett.* **44**(19), 4694–4697 (2019).
- V. Sharma, S. C. Kumar, G. Samanta, and M. Ebrahim-Zadeh, *Opt. Express* **30**(2), 1195–1204 (2022).
- V. Sharma, S. C. Kumar, G. Samanta, and M. Ebrahim-Zadeh, *Opt. Lett.* **46**(13), 3235–3238 (2021).
- J. Wang, J. Yang, I. M. Fazal, N. Ahmed, Y. Yan, H. Huang, Y. Ren, Y. Yue, S. Dolinar, M. Tur, and A. E. Willner, *Nat. Photonics* **6**(7), 488–496 (2012).
- M. Krenn, R. Fickler, M. Fink, J. Handsteiner, M. Malik, T. Scheidl, R. Ursin, and A. Zeilinger, *New J. Phys.* **16**(11), 113028 (2014).
- M. Krenn, J. Handsteiner, M. Fink, R. Fickler, R. Ursin, M. Malik, and A. Zeilinger, *Proc. Natl. Acad. Sci. U. S. A.* **113**(48), 13648–13653 (2016).
- A. Sit, F. Bouchard, R. Fickler, J. Gagnon-Bischoff, H. Larocque, K. Heshami, D. Elser, C. Peuntinger, K. Günthner, B. Heim *et al.*, *Optica* **4**(9), 1006–1010 (2017).
- S. Liu, Z. Zhou, S. Liu, Y. Li, Y. Li, C. Yang, Z. Xu, Z. Liu, G. Guo, and B. Shi, *Phys. Rev. A* **98**(6), 062316 (2018).
- R. Fickler, G. Campbell, B. Buchler, P. K. Lam, and A. Zeilinger, “Quantum entanglement of angular momentum states with quantum numbers up to 10,010,” *Proc. Natl. Acad. Sci. U. S. A.* **113**(48), 13642–13647 (2016).
- X. Wang, X. Cai, Z. Su, M. Chen, D. Wu, L. Li, N. Liu, C. Lu, and J. Pan, *Nature* **518**(7540), 516–519 (2015).

- <sup>35</sup>K. Zou, K. Pang, H. Song, J. Fan, Z. Zhao, H. Song, R. Zhang, H. Zhou, A. Minoofar, C. Liu, X. Su, N. Hu, A. McClung, M. Torfeh, A. Arbabi, M. Tur, and A. E. Willner, *Nat. Commun.* **13**(1), 7662 (2022).
- <sup>36</sup>N. Wang, S. Liu, R. Zhao, T. Xu, F. Chen, A. Arie, W. Krolikowski, and Y. Sheng, *Opt. Lett.* **47**(15), 3656–3659 (2022).
- <sup>37</sup>D. Liu, S. Liu, L. M. Mazur, B. Wang, P. Lu, W. Krolikowski, and Y. Sheng, *Appl. Phys. Lett.* **116**(5), 051104 (2020).
- <sup>38</sup>C. Zhang, C. Min, L. Du, and X.-C. Yuan, *Appl. Phys. Lett.* **108**(20), 201601 (2016).
- <sup>39</sup>H. Yan, E. Zhang, B. Zhao, and K. Duan, *Opt. Express* **20**(16), 17904–17915 (2012).
- <sup>40</sup>S. Rojas-Rojas, G. Cañas, G. Saavedra, E. S. Gómez, S. P. Walborn, and G. Lima, *Opt. Express* **29**(15), 23381–23392 (2021).
- <sup>41</sup>C. Brunet, P. Vaity, Y. Messaddeq, S. LaRochelle, and L. A. Rusch, *Opt. Express* **22**(21), 26117–26127 (2014).
- <sup>42</sup>S. Franke-Arnold, J. Leach, M. J. Padgett, V. E. Lembessis, D. Ellinas, A. J. Wright, J. M. Girkin, P. Öhberg, and A. S. Arnold, *Opt. Express* **15**(14), 8619–8625 (2007).
- <sup>43</sup>M. Chen, M. Mazilu, Y. Arita, E. M. Wright, and K. Dholakia, *Opt. Lett.* **38**(22), 4919–4922 (2013).
- <sup>44</sup>E. Otte and C. Denz, *Appl. Phys. Rev.* **7**(4), 041308 (2020).
- <sup>45</sup>G. Tkachenko, M. Chen, K. Dholakia, and M. Mazilu, *Optica* **4**(3), 330–333 (2017).
- <sup>46</sup>J. Řeháček, Z. Bouchal, R. Čechovský, Z. Hradil, and L. L. Sánchez-Soto, *Phys. Rev. A* **77**(3), 032110 (2008).
- <sup>47</sup>Z.-C. Ren, L. Fan, Z.-M. Cheng, Z.-F. Liu, Y.-C. Lou, S.-Y. Huang, C. Chen, Y. Li, C. Tu, J. Ding, X.-L. Wang, and H.-T. Wang, *Optica* **11**(7), 951–961 (2024).
- <sup>48</sup>Y. Chen, R. Ni, Y. Wu, L. Du, X. Hu, D. Wei, Y. Zhang, and S. Zhu, *Phys. Rev. Lett.* **125**(14), 143901 (2020).